Fumarate hydratase inhibits non-small cell lung cancer metastasis via inactivation of AMPK and upregulation of DAB2

ANUPAMA VADHAN[1], YI-FANG YANG[2], YUN-MING WANG[3-5], PANG-YU CHEN[1], SHEY-CHERNG TZOU[6-8], KUANG-HUNG CHENG[9,10], STEPHEN CHU-SUNG HU[11,12], TIAN-LU CHENG[8,13], YEN-YUN WANG[5,14] and SHYNG-SHIOU F. YUAN[1,3,14-16]

[1]Graduate Institute of Medicine, College of Medicine, Kaohsiung Medical University, Kaohsiung 807; [2]Department of Medical Education and Research, Kaohsiung Veterans General Hospital, Kaohsiung 813; [3]Department of Biological Science and Technology, Institute of Molecular Medicine and Bioengineering, Center for Intelligent Drug Systems and Smart Bio-devices (IDS²B), National Yang Ming Chiao Tung University, Hsinchu 300; [4]Department of Biomedical Science and Environmental Biology, Center for Cancer Research; [5]School of Dentistry, College of Dental Medicine, Kaohsiung Medical University, Kaohsiung 807; [6]Institute of Molecular Medicine and Bioengineering; [7]Department of Biological Science and Technology, National Yang Ming Chiao Tung University, Hsinchu 300; [8]Drug Development and Value Creation Research Center, Kaohsiung Medical University, Kaohsiung 807; [9]Institute of Biomedical Sciences, National Sun Yat-Sen University, Kaohsiung 804; [10]Department of Medical Laboratory Science and Biotechnology; [11]Department of Dermatology, College of Medicine, Kaohsiung Medical University; [12]Department of Dermatology, Kaohsiung Medical University Hospital; [13]Department of Biomedical and Environmental Biology, Kaohsiung Medical University; Departments of [14]Medical Research, [15]Translational Research Center, and [16]Obstetrics and Gynecology, Kaohsiung Medical University Hospital, Kaohsiung 807, Taiwan, R.O.C.

Abstract. Lung cancer is one of the leading causes of cancer mortality worldwide. As it is often first diagnosed only when cancer metastasis has already occurred, the development of effective biomarkers for the risk prediction of cancer metastasis, followed by stringent monitoring and the early treatment of high-risk patients, is essential for improving patient survival. Cancer cells exhibit alterations in metabolic pathways that enable them to maintain rapid growth and proliferation, which are quite different from the metabolic pathways of normal cells. Fumarate hydratase (FH, fumarase) is a well-known tricarboxylic acid cycle enzyme that catalyzes the reversible hydration/dehydration of fumarate to malate. The current study sought to investigate the relationship between FH expression levels and the outcome of patients with lung cancer. FH was knocked down in lung cancer cells using shRNA or overexpressed using a vector, and the effect on migration ability was assessed. Furthermore, the role of AMP-activated protein kinase (AMPK) phosphorylation and disabled homolog 2 in the underlying mechanism was investigated using an AMPK inhibitor approach. The results showed that in lung cancer tissues, low FH expression was associated with lymph node metastasis, tumor histology and recurrence. In addition, patients with low FH expression exhibited a poor overall survival in comparison with patients having high FH expression. When FH was overexpressed in lung cancer cells, cell migration was reduced with no effect on cell proliferation. Furthermore, the level of phosphorylated (p-)AMPK, an energy sensor molecule, was upregulated when FH was knocked down in lung cancer cells, and the inhibition of p-AMPK led to an increase in the expression of disabled homolog 2, a tumor suppressor protein. These findings suggest that FH may serve as an effective biomarker for predicting the prognosis of lung cancer and as a therapeutic mediator.

Introduction

Lung cancer is one of the most common causes of cancer-associated mortality globally (1). While tobacco smoking is the most frequent cause of lung cancer, numerous cases are also reported in nonsmokers that may be associated with various

---

Correspondence to: Dr Yen-Yun Wang, School of Dentistry, College of Dental Medicine, Kaohsiung Medical University, 100 Shih-Chuan 1st Road, Sanmin, Kaohsiung 807, Taiwan, R.O.C.
E-mail: wyy@kmu.edu.tw

Dr Shyng-Shiou F. Yuan, Graduate Institute of Medicine, College of Medicine, Kaohsiung Medical University, 100 Shih-Chuan 1st Road, Sanmin, Kaohsiung 807, Taiwan, R.O.C.
E-mail: yuanssf@kmu.edu.tw

alternative factors, including air pollution, environmental exposure, mutations and single-nucleotide polymorphisms (2). Lung cancer is classified histologically as small cell lung cancer (SCLC), which accounts for 15-20% of lung cancer cases, and non-SCLS (NSCLC) that accounts for ~80% of lung cancer cases and includes adenocarcinoma, large cell carcinoma and squamous cell carcinoma (3,4). Patients with both histological types have a poor prognosis, with a 5-year survival rate of only 15%. A thorough understanding of the contributing factors, differences in histopathology and molecular characteristics of lung cancer in smokers and nonsmokers, as well as the role played by various carcinogenic factors may facilitate the prevention and treatment of lung cancer (2,5).

Fumarate hydratase (FH) is a key enzyme in the tricarboxylic acid (TCA) cycle, which catalyzes the hydration of fumarate to form malate and is generally categorized as a tumor suppressor. The inactivation of FH causes its substrate fumarate to accumulate, enabling fumarate to leak out into the cytosol where it inhibits prolyl hydroxylase enzymes and stabilizes hypoxia-inducible factor 1, a mediator of glycolysis (6). A previous study demonstrated that the expression of FH mRNA is downregulated in A549 lung cancer cells compared with 16HBE non-tumorigenic bronchial epithelial cells, and the expression of FH determined by immunohistochemistry is significantly lower in lung cancer tissues than in normal lung tissues and is not associated with TNM status (7). In addition, a study by Chen *et al* (8) showed that the phosphorylation of FH at serine 46 by p21-activated kinase 4 promotes tumorigenesis in lung cancer by inhibiting the phosphorylation of FH at threonine 90.

Disabled homolog 2 (DAB2) is a tumor suppressor protein that is downregulated in various malignancies, including gastric (9), breast (10) and prostate cancer (11). In lung cancer, DAB2 is expressed at low levels (12) and hypermethylated (13,14). It is also a target of various microRNAs (miRs), which results in DAB2 downregulation in lung cancer (15,16).

AMP-activated protein kinase (AMPK) is an energy-sensing protein kinase that regulates energy metabolism in cells (17) and is activated by various cellular processes, including oxidative stress, changes in the AMP/ATP ratio and hypoxic conditions (18). AMPK has been reported to play a role in the proliferation, metastasis and drug resistance of lung cancer (19), and the activity of AMPK has been shown to be altered in the absence of FH (20).

The present study aimed to investigate the association of FH expression levels with the outcome of patients with lung cancer. Furthermore, FH was knocked down in lung cancer cells using short hairpin RNA (shRNA) or overexpressed using a vector and the effect on migration ability was evaluated. In addition, the potential involvement of AMPK phosphorylation and DAB2 in the underlying mechanism was investigated. It is hoped that the findings of the study may provide insights to aid the development of novel strategies for lung cancer treatment.

Materials and methods

Oncomine database analysis. The expression level of FH in lung adenocarcinoma tissue compared with normal lung tissue was analyzed using the Oncomine online database (https://www.oncomine.org).

Patient samples. Lung cancer tissues were obtained from patients undergoing surgical treatment at Kaohsiung Medical University Hospital (Kaohsiung, Taiwan) and E-Da Hospital (Kaohsiung, Taiwan) between February 2007 and February 2013. All patients with lung cancer (adenocarcinoma and squamous cell carcinoma) who underwent a lung resection, including 68 men and 36 women, were included in the study. The age distribution was from 29 to 84 years old. Patients with diseases other than lung cancer were excluded. Overall survival (OS) was defined as the interval between the date of diagnosis and death. IRB approval was received from the Institutional Review Board (or Ethics Committee) of Kaohsiung Medical University Hospital [KMUHIRB-E(I)-20180026] and the Institutional Review Board for Human Studies of E-Da Hospital (EMRP-098-132 and EMRP-101-040). Written informed consent was obtained from all the patients.

Tissue microarray and immunohistochemistry. All tissues used to create the tissue microarray were obtained from formalin-fixed, paraffin-embedded tissue blocks. Histopathological slides prepared from hematoxylin and eosin-stained sections were evaluated by a pathologist who selected representative areas of tumor or normal tissues for scoring. The tissue microarray was constructed using Booster Arrayer & TMA designer software (Alphelys) according to a previously described procedure (21).

The immunohistochemical (IHC) staining of FH was performed using a Bond-Max automated system (Leica Microsystems GmbH) with an anti-FH antibody (GTX110128; 1:500; GeneTex, Inc.). The relative expression of FH in the lung cancer specimens was quantified using a TissueFAXS microscopy system and HistoQuest software 2.0 (TissueGnostics GmbH). The IHC score of the lung cancer tissue was calculated by multiplying the percentage (1-100%) of positively stained cells by the intensity of staining (0, 1+, 2+ or 3+). For further statistical analysis, low and high expression categories were established based on a receiver operating characteristic curve analysis. Patients with lung cancer were classified into two groups using the these scoring categories as follows: Low FH, IHC score <45; and high FH, IHC score ≥45.

Cell culture. The CL1-0, H441, H1299 and CL1-5 human lung cancer cell lines were purchased from the Bioresource Collection and Research Center and were maintained in Roswell Park Memorial Institute (RPMI)-1640 medium (Gibco; Thermo Fisher Scientific, Inc.). A549, H250 and H460 cells were purchased from the American Type Cell Collection and maintained in RPMI-1640 medium. All cell lines were cultured with 5% CO_2 at 37˚C in a humdified incubator. All culture media were supplemented with 10% fetal bovine serum (FBS; Biological Industries) and 1% penicillin G, streptomycin and amphotericin B.

Virus infection for FH knockdown or overexpression. For the knockdown of FH in the CL1-0 and H441 lung cancer cell lines, a pLKO.1_puro lentiviral vector (National RNAi Core Facility Platform, Academia Sinica) expressing double-stranded shRNA oligonucleotides targeting human FH (2 clones) was used: Clone 1 (shFH1), IDTRCN0000052466, target sequence, 5'-GTGGTTATGTTCAACAAGTAA-3' and

oligo sequence: 5'-CCGGGTGGTTATGTTCAACAAGTA ACTCGAGTTACTTGTTGAACATAACCACTTTTTG-3'; and clone 2 (shFH2), ID TRCN0000310398, target sequence, 5'-CCCAACGATCATGTTAATAAA-3' and oligo sequence, 5'-CGGCCCAACGATCATGTTAATAAACTCGAGTTT ATTAACATGATCGTTGGGTTTTTG-3' (National RNAi Core Facility, Academia Sinica). A pLKO.1_puro lentiviral vector expressing shRNA targeting firefly luciferase (shluc), which is not associated with the human genome sequence, was used as a negative control (National RNAi Core Facility, Academia Sinica). For the overexpression of FH in H1299 cells, a lentivirus with a pLVX-puro backbone (#GRVL7005G) and empty control (#GRV7006G) were purchased from Topgen Biotechnology Co., Ltd. Cell infection was performed according to the detailed procedures described in a previous study (22).

Transwell migration and invasion assays. Cell migration assays were carried out using Transwell (Costar; Corning Inc.) membrane filter inserts (diameter, 6.5 mm; pore size, 8 μm) in 24-well tissue culture plates. Following the knockdown or overexpression of FH, CL1-0, H441 and H1299 lung cancer cells were trypsinized, suspended in serum-free RPMI 1640 medium and seeded ($2x10^4$ cells) on the Transwell filter in the upper chamber, while RPMI-1640 medium containing 10% FBS (Biological Industries) was added to the lower chamber. The cells were then incubated for 24 h at 37°C. After incubation, the cells were fixed with 4% formaldehyde for 10 min and stained with crystal violet for 2 h, at room temperature. Non-migrating cells were removed by wiping the upper side of the filter, and the migrated cells were imaged using Olympus SZX10 stereo light microscope (Olympus Corporation) and analyzed using ImageJ software (ij153-win-java8; National Institutes of Health).

BioCoat Matrigel invasion chambers (Corning Inc.) were used for the invasion assay. Prior to use, Transwell invasion chambers were rehydrated with serum-free medium for 2 h. The remainder of the protocol was identical to that of the migration assay, with the exception that the lung cancer cells were not transfected. ImageJ software was used to count the number of invaded cells. The invasive ability was calculated based on the percentage of invaded cells and normalized to CL1-5.

Western blotting. Western blot analysis was performed to check the knockdown and overexpression efficiency of lentivirus infection and to evaluate the expression of other proteins in the cells using a previously described procedure (23). Antibodies against FH (#GTX110128; 1:2,000; GeneTex, Inc.), p-AMPK (GTX52341; 1,1,000; GeneTex, Inc.), AMPK (#5831; 1:1,000; Cell Signaling Technology, Inc.), DAB2 (AF8064; 1:500; R&D Systems, Inc.), jagged canonical Notch ligand 1 (JAG1; GTX31607; 1:1,000; GeneTex, Inc.), interferon-related developmental regulator 1 (IFRD1; GTX104578; 1:1,000; GeneTex, Inc.) and actin (#A5441; 1:5,000; MilliporeSigma) were used. The AMPK inhibitor BML-275 was purchased from Santa Cruz Biotechnology, Inc. (sc-200689). H441 cells were treated with BML-275 (15 μM) for 24 h at 37°C in 1% FBS-containing medium before collection for western blot analysis. In brief, after protein transfer, the polyvinylidene fluoride (PVDF)

membrane was incubated overnight at 4°C with primary antibodies, followed by incubation with secondary rabbit (HRP conjugate; GTX2131101; 1:5,000; GeneTex, Inc.) or mouse (HRP conjugate; GTX213111; 1:5,000; GeneTex, Inc.) antibodies for 1 h at room temperature. The protein bands on the PVDF membrane were visualized using Western Lightning[R] Plus-ECL enhanced chemiluminescence substrate (PerkinElmer, Inc.) and analyzed using Image Lab software 6.0.1 (Bio-Rad Laboratories, Inc.).

Cell proliferation assay. A cell proliferation assay was performed using 2,3-bis-(2-methoxy-4-nitro-5-sulfophenyl)-2H-tetrazolium-5-carboxanilide (XTT) as described in previous studies (24,25). In brief, H441, CL1-0 and H1299 cells were seeded in 96-well plates (3,000 cells/well). After 24-72 h, XTT (X4251; Sigma-Aldrich; Merck KGaA) solution containing phenazine methosulfate (P9625; Sigma-Aldrich; Merck KGaS) was added. After 30 min, the absorbance was measured at 475 and 660 nm. The proliferation rate was calculated as 475 nm absorbance minus non-specific reading at 660 nm absorbance.

Metabolic profile analysis. Following the knockdown of FH, CL1-0 lung cancer cells were seeded ($1x10^6$ cells/plate) in a 10-mm dish. After 24 h, the medium was removed and the cells were washed with PBS twice. The PBS was removed and 1 ml ice-cold methanol diluted with water (80:20) was added in accordance with a previously described method (26). The cells were scraped from the dish and transferred to Eppendorf tubes, in which the mixture was vortexed and put on ice for 5 min. The samples were then centrifuged at 18,528 x g at 4°C for 10 min, and the supernatants were collected into clean Eppendorf tubes and subjected to speed vacuum concentration followed by lyophilization to obtain the samples in powdered form. Metabolic data were acquired from the samples using a Q Exactive™ Plus Orbitrap Mass Spectrometer (Thermo Fisher Scientific, Inc.) coupled with a Vanquish™ UPLC (Thermo Fisher Scientific, Inc.) under John Hopkins University (Baltimore, USA) metabolomics analysis service. All metabolomics data were normalized by the protein concentration of each sample. Multiple reaction monitoring for fumarate and malate was assessed at the mass transitions 115 to 100 and 133.01 to 100 m/z, respectively, with a retention time of 4 min. Other parameters were as follows: Negative ionization mode of detection, 350°C nitrogen gas temperature, 35 psi nebuliser pressure and an 11 l/min sheath gas flow rate.

RT² profiler PCR array. TRIzol® reagent (Thermo Fisher Scientific, Inc.) was used to extract total RNA from the FH knockdown CL1-0 cells and the respective shluc control cells in accordance with the manufacturer's instructions. An aliquot of RNA (2 g/sample) was processed with DNase (Merck &Co., Inc.) and converted into cDNA using an RT2 First Strand Kit (Qiagen, Inc.). Then, using the human-signal transduction pathway finder RT² profiler PCR array (PAHS-014Z; Qiagen, Inc.), 84 pathway-associated genes and 5 housekeeping genes were screened according to the manufacturer's instructions.

Statistical analysis. All statistical analyses were performed using the SPSS 14.0 statistical package for PC (SPSS, Inc.).

Comparisons between two groups were performed using unpaired Student's t-test while comparisons among multiple groups were performed using one-way ANOVA followed by Tukey's post hoc test. The relationship between the expression of FH and invasive ability was evaluated by linear regression. Associations of the expression of FH with age, sex, stage, tumor size, lymph node metastasis, distant metastasis, histologic type, tumor recurrence and smoking status were investigated by χ^2 or Fisher's exact tests. Survival curves were generated using Kaplan-Meier estimates and the significance of difference between curves was evaluated by log-rank test. Furthermore, univariate and multivariate Cox regression models were used to investigate the associations between clinicopathological characteristics and OS. P<0.05 was considered to indicate a statistically significant result.

Results

FH expression is associated with prolonged survival in lung cancer patients. Assessment of the FH expression level in patients with lung cancer using the Oncomine database revealed that FH mRNA expression was significantly lower in lung adenocardinoma tissues compared with normal lung tissues (Fig. 1A). Furthermore, the protein expression levels of FH in lung cancer tissues collected from patients were analyzed by IHC staining (Fig. 1B). The results showed that lung cancer tissue had lower expression of FH compared with normal lung alveoli. Survival analysis of the patients with lung cancer revealed that the OS of the high FH expression group was significantly prolonged compared with that of the low FH expression group (P=0.029; Fig. 1C).

The associations between FH expression levels and the clinicopathological characteristics of the patients with lung cancer were also examined. The results revealed that low FH expression was significantly associated with lymph node metastasis (P=0.028) and disease recurrence (P=0.05) (Table I). Although the multivariate analysis did not show that FH expression level was a significant factor for OS (P=0.093), the univariate analysis indicated that FH expression level was a significant predictor of OS for patients with lung cancer (P=0.013; Table II), and high FH expression was associated with lower hazard ratio.

FH inhibits the migration ability of lung cancer cells. The analysis of the clinicopathological data indicated that FH might play an important role in lung cancer metastasis (Table I). Therefore, the effect of FH on lung cancer cell invasion and migration was investigated *in vitro*. Western blotting showed that the level of endogenous FH was downregulated in highly invasive CL1-5, H1299 and A549 cells, and FH expression was negatively associated with invasion ability in seven human lung cancer cell lines (Figs. 2A, B and S1). Knockdown of FH expression in the poorly invasive CL1-0 and H441 lung cancer cell lines significantly increased the migration ability of the cells compared with the respective shluc-transfected control cells (Fig. 2C). To ensure that the knockdown of FH had an effect on the TCA cycle and reduced FH activity, the fumarate level in FH knockdown CL1-0 cells was also measured by metabolomics analysis and the results revealed that fumarate level was significantly higher while the malate level was significantly lower
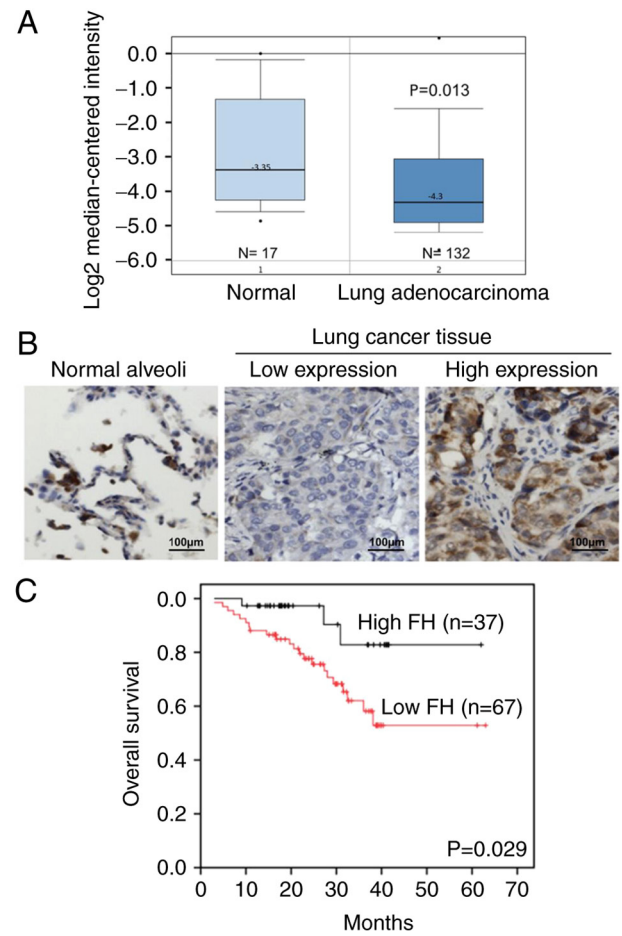
Figure 1. Expression of FH and the association of FH with clinical outcomes in patients with lung cancer. (A) mRNA expression level of FH in normal lung tissues and lung cancer tissues analyzed using the Oncomine online database. (B) Protein expression of FH determined by immunohistochemistry in normal lung tissues and lung cancer tissues collected from patients. (C) Overall survival of patients with lung cancer according to their FH expression levels. FH, fumarate hydratase.

in the FH knockdown cells compared with the shluc control (Fig. S2). Conversely, the overexpression of FH in the highly invasive H1299 cell line significantly reduced the migration ability of the cells compared with the control cells (Fig. 2D). This supported the patient data which showed that low FH expression was significantly associated with lymph node metastasis in lung cancer. The XTT assay showed that the neither the knockdown nor the overexpression of FH in lung cancer cells affected the proliferative potential of the cells (Fig. 2E).

FH knockdown downregulates DAB2 expression and upregulates AMPK phosphorylation. The human-signal transduction pathway finder RT² profiler PCR array was used to investigate the downstream and upstream genes in FH knockdown CL1-0 cells. The results showed that three mRNAs, namely IFRD1 (fold change 2.03), JAG1 (fold change 2.35) and DAB2 (fold change-2.37) showed >2-fold changes in the FH knockdown group compared with the control group (Fig. 3A and B). These findings were evaluated at the protein level by western blotting and the results confirmed that DAB2 protein expression in FH knockdown cells CL1-0 and H441 was downregulated by 0.3 and 0.4 fold, respectively, compared

Table I. Association of FH expression with clinicopathological characteristics in patients with lung cancer.

| | FH | | |
	Low (<45), n	High (≥45), n	P-value[a]
Variables			
Patients	67	37	
Age (years)			0.071
≤70	43	30	
>70	24	7	
Sex			0.934
Female	23	13	
Male	44	24	
Stage			0.100
I/II	42	29	
III/V	25	8	
T status			0.861
T1/T2	57	31	
T3/T4	10	6	
N status			0.028
Negative	36	28	
Positive	31	9	
M status			0.489[b]
Negative	59	35	
Positive	8	2	
Histology			0.023
Adenocarcinoma	49	34	
Squamous cell carcinoma	18	3	
Recurrence			0.05
No	30	24	
Yes	37	13	
Smoking status			0.683
Never	38	24	
Former	15	6	
Current	14	7	

[a]P-values were calculated using χ^2 test unless otherwise specified; [b]P-value was determined by Fisher's exact test.

with the shluc control group. By contrast, DAB2 protein level in FH overexpressed cells was upregulated by 1-fold, compared with the vector control (Fig. 3C). However, IFRD1 and JAG1 protein expression did not change following FH knockdown in the same manner as the mRNA expression observed in the RT² array analysis. (Fig. S3). Therefore, DAB2 was focused upon for further experiments.

Previous studies have shown that fumarate accumulation affects AMPK protein expression. For example, in kidney cancer, FH deficiency has been reported to downregulate AMPK expression (20). Also, in renal cancer cells, it has been reported that fumarate activates AMPK, which protects FH-deficient cancer cells from apoptosis (27). Therefore, AMPK and p-AMPK protein levels were evaluated by western blotting. The results demonstrated that p-AMPK protein levels were upregulated in FH knockdown CL1-0 and H441 cells by 2- and 1.5-fold, respectively, compared with the control shluc group (Fig. 3C) while p-AMPK protein levels were downregulated in FH overexpressing H1299 cells by 0.7-fold (Fig. 3C). Furthermore, to investigate whether DAB2 was downstream or upstream of p-AMPK, FH knockdown H441 cells were treated with the p-AMPK inhibitor BML-275. Western blotting demonstrated that the inhibition of p-AMPK upregulated DAB2 protein expression by 1.5-fold in FH knockdown cells (Fig. 3D). These results suggest that the downregulation of FH leads to an increase in AMPK phosphorylation, which decreases DAB2 protein expression, resulting in increased cancer cell motility (Fig. 3E).

Discussion

FH has been shown to play a role in uterine leiomyoma, soft tissue sarcomas and type II papillary renal cell carcinoma (28-31), and the accumulation of fumarate has been shown to promote various signaling pathways and metabolic changes in cancer, particularly renal cancer (32-36). However, the role of FH in lung cancer has not been studied extensively. Accordingly, the present study was performed to investigate the potential function of FH in lung cancer.

Initially, the analysis of an online dataset in the Oncomine database indicated that the expression of FH was lower in lung cancer tissue compared with normal tissue. Therefore, the expression of FH was evaluated in lung cancer tissue samples collected from patients and it was observed that lung cancer tissue had low expression levels of FH when compared with normal alveoli. A survival analysis revealed that patients with lung cancer who had high FH expression had an improved OS when compared with those with low FH expression. The findings of the present study are similar those in a previous study on lung cancer by Ming et al (7), which suggested that the low expression of FH could be an indicator of tumorigenesis, while the present study found that the expression of FH was negatively associated with lymph node metastasis and cancer recurrence. As lung cancer is more common in Taiwanese males than females, the proportion of males was higher than that of females in the present study. Similar sex ratios have been reported in previous studies (37,38).

The results of the present study showed that the migration ability of lung cancer cells was increased while cell proliferation was not affected when FH was knocked down, suggesting a suppressive role of FH in metastasis. These findings are consistent with those of studies by Sciacovelli et al (30,39), which reported that accumulation of fumarate without conversion to malate by FH promoted epithelial-to-mesenchymal transition in renal cancer. Also, the low expression level of FH in lung cancer cells implies that FH might be a tumor suppressor (7). Intriguingly, the phosphorylation of FH at threonine-90 has been shown to induce the growth arrest of lung cancer cells (40). Whether this phosphorylation site of FH contributes to the FH-mediated metastasis of lung cancer cells remains to be investigated.

Table II. Univariate and multivariable analysis of overall survival for patients with lung cancer.

Variables	Univariate			Multivariate[a]		
	HR	95% CI	P-value	HR	95% CI	P-value
Age (years)	1.52	(0.68, 3.39)	0.302	-	-	-
>70						
≤70	1.00			-		
Sex						
Male	1.46	(0.46, 4.47)	0.523	-	-	-
Female	1.00			-		
T status						
T3/T4	1.11	(0.25, 4.96)	0.893	-	-	-
T1/T2	1.00			-		
N status						
Positive	5.45	(2.22, 13.37)	0.010	4.56	(1.84, 11.3)	0.001
Negative	1.00			1.00		
M status						
Positive	3.37	(1.34, 8.45)	0.010	2.29	(0.88, 5.95)	0.089
Negative	1.00			1.00		
Histology						
Squamous cell carcinoma	1.56	(0.62, 3.92)	0.345	-	-	-
Adenocarcinoma	1.00			-		
Smoking status						
Current	2.11	(0.79, 6.05)	0.130	-	-	-
Former	2.83	(1.73, 7.14)	0.021	-		
Never	1.00					
FH						
High	0.27	(0.08, 0.90)	0.013	0.35	(0.10, 1.19)	0.093
Low	1.00			1.00		

[a]Variables with P<0.1 were included in the multivariate analysis. HR, hazard ratio; CI, confidence interval; -, not applicable; FH, fumarate hydratase.

Using the human-signal transduction pathway finder RT^2 array, it was found that the DAB2 mRNA level was decreased and JAG1 and IFRD1 mRNA levels were increased in FH knockdown cells; however, the expression levels of JAG1 and IFRD1 proteins as determined by western blotting did not follow the same trends as those obtained from the RT^2 array. One possible explanation for the discrepancy between JAG1 and IFRD1 mRNA and protein expression trends is post-transcriptional modification. For example, small non-coding RNAs can perform post-transcriptional modifications by binding to the mature RNA of a target gene via the RNA-induced silencing complex, which causes the destruction of the mRNA and/or the suppression of translation (41). However, further investigations are required to fully explain these discrepant results.

Previous research has shown that the downregulation of DAB2 promotes migration in various cancers. Specifically, in breast cancer, the knockdown of DAB2 promotes cancer cell migration via increased Ras/MAPK signaling and the development of an autocrine transforming growth factor signaling loop, which further promotes epithelial-mesenchymal transition (42). In addition, the downregulation of DAB2 in gastric cancer activates Wnt/β-catenin and Hippo/YAP signaling pathways, which further downregulate the expression of the epithelial marker E-cadherin and upregulate the expression of the mesenchymal markers MMP2 and MMP9 to promote cancer cell migration (9). Furthermore, DAB2 is suppressed by miR-106b and miR-134-5p directly binding to the 3' untranslated region of DAB2 in hepatocellular carcinoma and lung cancer cells, respectively, which results in the upregulation of cell migration (16,43). These studies support the finding that the downregulation of DAB2 in FH knockdown cells is associated with lung cancer cell migration.

AMPK has been implicated in the progression of lung cancer in numerous studies and has been shown to promote lung cancer metastasis by activating various upstream mediators. In a previous study, the inositol monophosphatase domain-containing 1-mediated activation of AMPK and its downstream effectors HEY1 and NOTCH1 was shown to promote lung cancer metastasis (44). Other studies
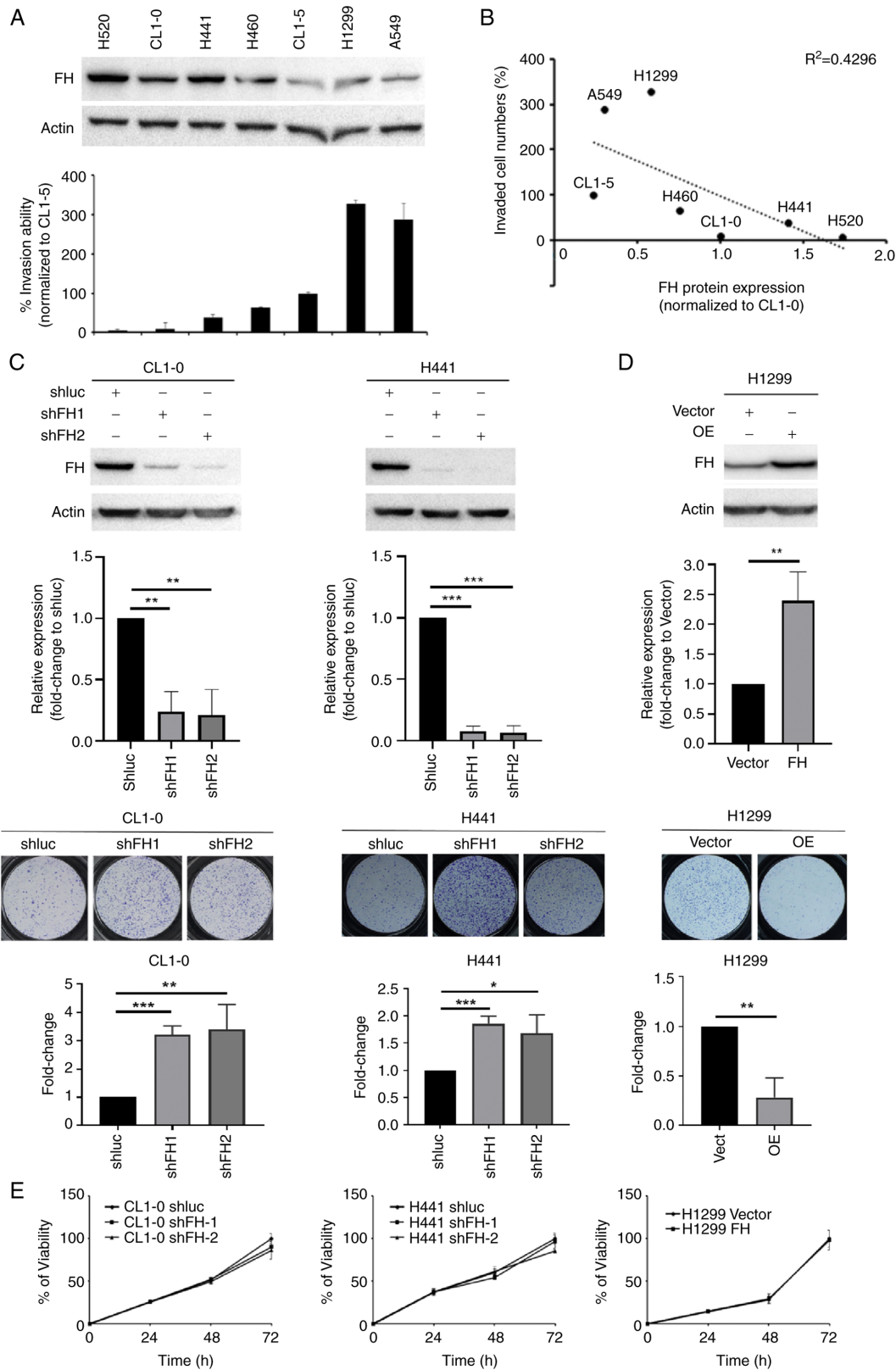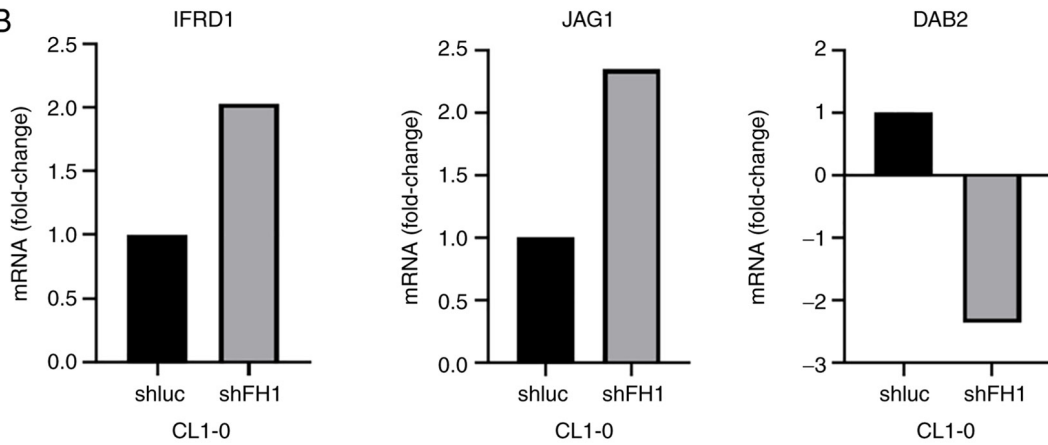
Figure 2. FH inhibits the migration ability of lung cancer cells. (A) Western blot analysis of endogenous FH in human lung cancer cell lines above a graph showing the invasive ability of the cells as evaluated using a Transwell invasion assay. (B) Relationship between FH expression and the invasion ability of lung cancer cell lines as determined by linear regression. (C) Effect of FH knockdown on the migration ability of CL1-0 and H441 lung cancer cells. Upper images show the western blotting of FH following lentiviral-mediated knockdown, with bar graph showing quantification of the western blotting data, and the lower images show the migration ability of CL1-0 and H441 cells after infection with shFH or shluc. Data are presented as the mean ± SD and were analyzed using one-way ANOVA followed by Tukey's post hoc test. $^*P<0.05$, $^{**}P<0.001$ and $^{***}P<0.0001$. (D) Effect of FH overexpression on the migration potential of H1299 lung cancer cells. Upper images show the western blot analysis of FH expression after FH overexpression compared with vector control, with the bar graph showing the quantification of the western blotting data, and the lower images show H1299 migration ability after FH overexpression. Data are presented as the mean ± SD and were analyzed using unpaired Student's t-test. $^{**}P<0.01$. (E) Cell proliferation in CL1-0 and H441 cells infected with shluc or shFH and in H1299 cells infected with FH overexpression vector or vector control. All experiments were performed three times independently. FH, fumarate hydratase; shFH, short hairpin RNA targeting FH; shluc, shRNA targeting firefly luciferase.

A

| Layout	1	2	3	4	5	6	7	8	9	10	11	12
A	ACSL3 -1.07	ACSL4 -1.32	ACSL5 -1.06 C	ADM -1.04	ARNT 1.11	ATF4 1.12	AXIN2 -1.04	BAX -1.02	BBC3 -1.02	BCL2 -3.04 A	BCL2A1 -1.06 C	BCL2L1 1.12
B	BIRC3 -1.25	BMP2 -1.06 C	BMP4 -1.14	BTG2 1.10	CA9 -1.06 C	CCL5 -1.24 B	CCND1 1.10	CCND2 1.06	CDKN1A 1.49	CDKN1B 1.03	CEBPD 1.30	CPT2 1.18
C	CSF1 2.10 B	DAB2 -2.37	EGFR -1.42	EMP1 -1.10	EPO -1.06 C	FABP1 1.27 B	FAS -1.06 C	FCER2 -1.57	FOSL1 -1.39	FTH1 -1.15	GADD45A 1.75	GADD45B 1.23
D	GATA3 1.26	GCLC -1.21	GCLM 1.04	GSR -1.23	HERPUD1 1.64	HES1 1.27	HES5 -1.06 C	HEY1 1.04	HEY2 1.76	HEYL 1.16	HMOX1 1.05	ICAM1 1.81 A
E	ID1 1.01	IFNG -1.06 C	IFRD1 2.03	IRF1 1.22	JAG1 2.35	LDHA -1.07	LFNG -1.55	LRG1 1.25 B	MCL1 1.21	MMP7 -1.06 C	MYC 1.15	NOTCH1 -1.16
F	NQO1 -1.08	OLR1 1.18	PCNA -1.10	PPARD 1.00	PTCH1 1.18	RB1 1.10	SERPINE1 -1.20 B	SLC27A4 -1.03	SLC2A1 -1.01	SOCS3 -1.40	SORBS1 1.18	SQSTM1 1.81
G	STAT1 -1.05	TNF -1.06 C	TNFSF10 -1.53 B	TXN -1.04	TXNRD1 1.09	VEGFA 1.40	WISP1 -1.06 C	WNT1 -1.06 C	WNT2B 1.20	WNT3A -1.39 B	WNT5A -1.48	WNT6 -1.06 C
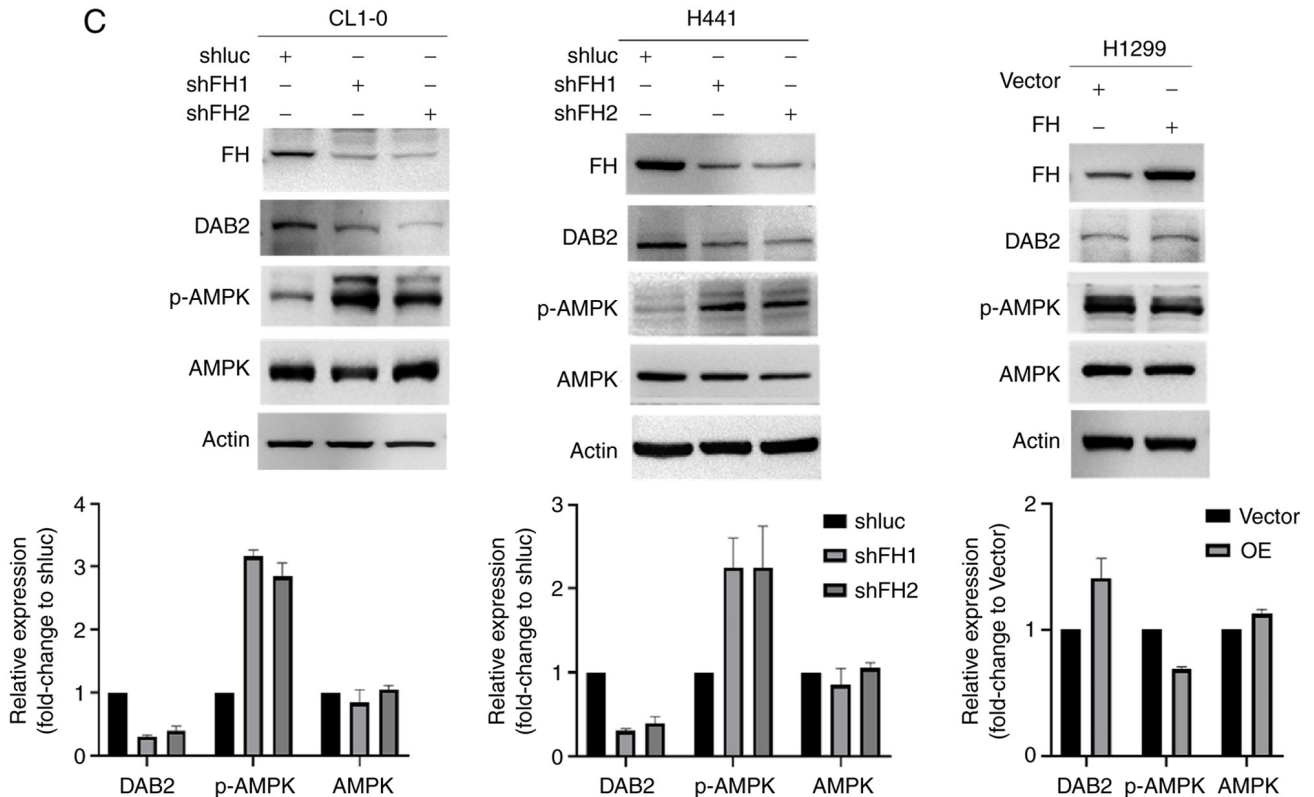
Figure 3. Continued.
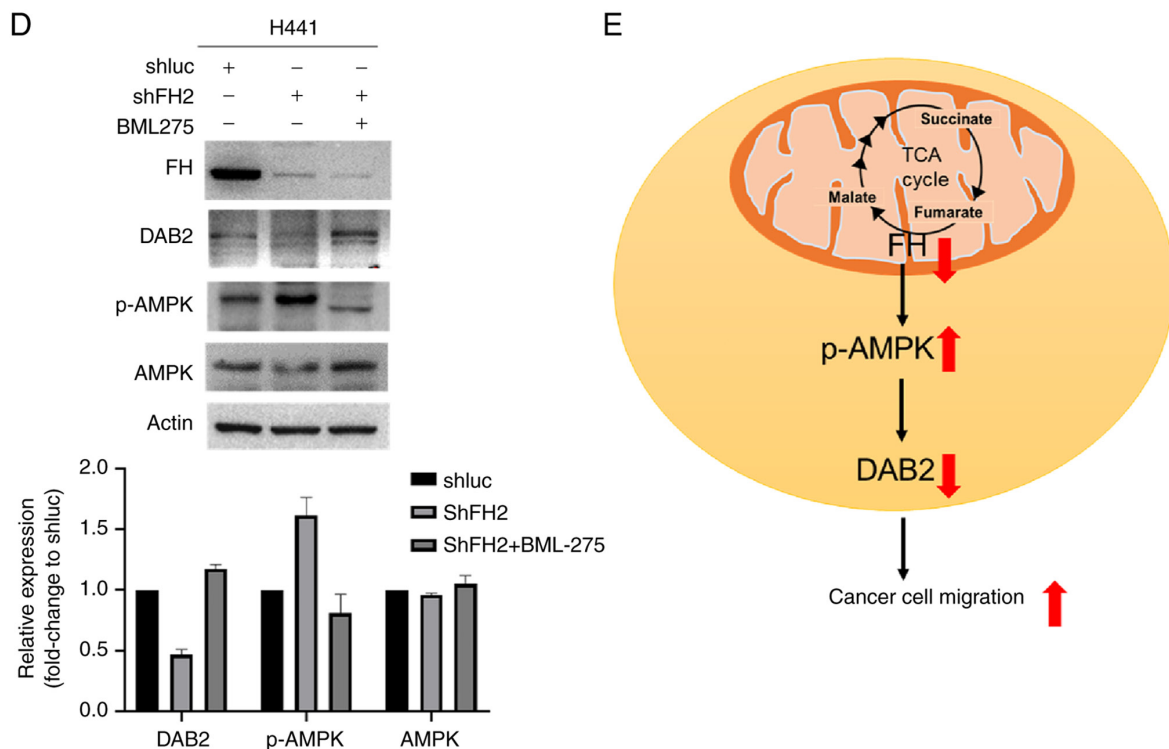
Figure 3. FH knockdown upregulates AMPK phosphorylation and downregulates DAB2 expression. (A) DAB2 was downregulated in FH knockdown cells, as identified by using the human signal transduction pathway finder RT² profiler PCR array. (B) Bar graphs showing the fold change in IFRD1, JAG1 and DAB2 mRNA levels compared with the shluc control group based on the RT² profiler PCR array results. Western blots showing FH, DAB2, p-AMPK, and AMPK protein expression in (C) FH knockdown CL1-0 and H441 cells and FH overexpressing H1299 cells and (D) H441 cells treated with 15 μM BML75 (in 1% FBS containing medium, 24 h). (E) Schematic diagram of the FH signaling pathway in lung cancer cells. All western blots were performed twice independently. FH, fumarate hydratase; shFH, short hairpin RNA targeting FH; shluc, shRNA targeting firefly luciferase; DAB2, disabled homolog 2; IFRD1, interferon-related developmental regulator 1; JAG1, jagged canonical Notch ligand 1; p-, phosphorylated; TCA, tricarboxylic acid cycle.

demonstrated that the activation of AMPK promotes the nuclear translocation of β-catenin, resulting in lung cancer metastasis (45,46). The present study demonstrated that the downregulation of FH promotes AMPK phosphorylation and contributes to lung cancer migration. We hypothesize that in lung cancer cells, the phosphorylation of AMPK might be increased due to mitochondrial dysfunction caused by FH knockdown (47). miR-451 has been reported to regulate AMPK expression in glioma cells by targeting AMPK partner LKB1 (48). It is possible that FH knockdown downregulates the level of miR-451 and leads to the upregulation of AMPK activity, but further investigations are required to verify this possibility. AMPK has been reported to function as an epigenetic regulator and so AMPK might promote DAB2 downregulation by its hypermethylation (49), as suggested by a previous study which showed that DAB2 is hypermethylated in non-small cell lung cancer (14). However, the current study focused on FH protein expression rather than the mutation status of FH in lung cancer.

Further studies are required to determine whether the inhibition of AMPK phosphorylation reverses the migration ability of lung cancer cells. Furthermore, the effect of FH knockdown on the extracellular acidification rate and oxygen consumption rate of lung cancer cells are important aspects that require further investigation, and the *in vitro* results require confirmation by *in vivo* modeling. However, in conclusion, the current study demonstrated that the low expression of FH promotes the migration of lung cancer cells via a mechanism involving AMPK signaling and DAB2 downregulation.

Availability of data and materials

The datasets used and/or analyzed during the current study are available from the corresponding author on reasonable request.

Authors' contributions

YFY, YYW and SSFY designed the study. AV, YFY and PYC performed the experiments and the formal analysis. YMW, SCT, KHC, SCSH, TLC, YYW, and SSFY investigated and validated the results. AV, YFY and PYC prepared and wrote the original draft of the manuscript. YMW, SCT, KHC, SCSH, TLC, YYW and SSFY reviewed and edited the manuscript. All authors read and approved the final version of the manuscript. AV and SSFY confirm the authenticity of all the raw data.

Ethics approval and consent to participate

The study was conducted in accordance with the Declaration of Helsinki and approved by the Institutional Review Board of Kaohsiung Medical University Hospital [KMUHIRB-E(I)-20220014] and the Institutional Review Board for Human Studies of the E-Da Hospital (EMRP-098-132 and EMRP-101-040). Written informed consent was obtained from all the patients.

Patient consent for publication

Not applicable.

Competing interests

The authors declare that they have no competing interests.

References

1. Sung H, Ferlay J, Siegel RL, Laversanne M, Soerjomataram I, Jemal A and Bray F: Global cancer statistics 2020: GLOBOCAN estimates of incidence and mortality worldwide for 36 cancers in 185 countries. CA Cancer J Clin 71: 209-249, 2021.
2. Akhtar N and Bansal JG: Risk factors of lung cancer in nonsmoker. Curr Probl Cancer 41: 328-339, 2017.
3. Ihde DC: Chemotherapy of lung cancer. N Engl J Med 327: 1434-1441, 1992.
4. Hoffman PC, Mauer AM and Vokes EE: Lung cancer. Lancet 355: 479-485, 2000.
5. Gou LY, Niu FY, Wu YL and Zhong WZ: Differences in driver genes between smoking-related and non-smoking-related lung cancer in the Chinese population. Cancer 121: 3069-3079, 2015.
6. King A, Selak MA and Gottlieb E: Succinate dehydrogenase and fumarate hydratase: Linking mitochondrial dysfunction and cancer. Oncogene 25: 4675-4682, 2006.
7. Ming Z, Jiang M, Li W, Fan N, Deng W, Zhong Y, Zhang Y, Zhang Q and Yang S: Bioinformatics analysis and expression study of fumarate hydratase in lung cancer. Thoracic Cancer 5: 543-549, 2014.
8. Chen T, Wang T, Liang W, Zhao Q, Yu Q, Ma CM, Zhuo L, Guo D, Zheng K, Zhou C, *et al*: PAK4 phosphorylates fumarase and blocks TGFβ-induced cell growth arrest in lung cancer cells. Cancer Res 79: 1383-1397, 2019.
9. Wang H, Dong S, Liu Y, Ma F, Fang J, Zhang W, Shao S, Shen H and Jin J: DAB2 suppresses gastric cancer migration by regulating the Wnt/β-catenin and Hippo-YAP signaling pathways. Transl Cancer Res 9: 1174-1184, 2020.
10. Tian X and Zhang Z: miR-191/DAB2 axis regulates the tumorigenicity of estrogen receptor-positive breast cancer. IUBMB Life 70: 71-80, 2018.
11. Hocevar BA: Loss of disabled-2 expression in pancreatic cancer progression. Sci Rep 9: 7532, 2019.
12. Xu HT, Yang LH, Li QC, Liu SL, Liu D, Xie XM and Wang EH: Disabled-2 and Axin are concurrently colocalized and underexpressed in lung cancers. Hum Pathol 42: 1491-1498, 2011.
13. Xie XM, Zhang ZY, Yang LH, Yang DL, Tang N, Zhao HY, Xu HT, Li QC and Wang EH: Aberrant hypermethylation and reduced expression of disabled-2 promote the development of lung cancers. Int J Oncol 43: 1636-1642, 2013.
14. Li C, Chen J, Chen T, Xu Z, Xu C, Ding C, Wang Y, Lei Z, Zhang HT and Zhao J: Aberrant hypermethylation at sites-86 to 226 of DAB2 gene in non-small cell lung cancer. Am J Med Sci 349: 425-431, 2015.
15. Du L, Zhao Z, Ma X, Hsiao TH, Chen Y, Young E, Suraokar M, Wistuba I, Minna JD and Pertsemlidis A: miR-93-directed downregulation of DAB2 defines a novel oncogenic pathway in lung cancer. Oncogene 33: 4307-4315, 2014.
16. Zhang L, Huang P, Li Q, Wang D and Xu CX: miR-134-5p promotes stage I lung adenocarcinoma metastasis and chemoresistance by targeting DAB2. Mol Ther Nucleic Acids 18: 627-637, 2019.
17. Hardie DG: AMPK-sensing energy while talking to other signaling pathways. Cell Metab 20: 939-952, 2014.
18. Kahn BB, Alquier T, Carling D and Hardie DG: AMP-activated protein kinase: Ancient energy gauge provides clues to modern understanding of metabolism. Cell Metab 1: 15-25, 2005.
19. Ashrafizadeh M, Mirzaei S, Hushmandi K, Rahmanian V, Zabolian A, Raei M, Farahani MV, Goharrizi MASB, Khan H, Zarrabi A and Samarghandian S: Therapeutic potential of AMPK signaling targeting in lung cancer: Advances, challenges and future prospects. Life Sci 278: 119649, 2021.
20. Tong WH, Sourbier C, Kovtunovych G, Jeong SY, Vira M, Ghosh M, Romero VV, Sougrat R, Vaulont S, Viollet B, *et al*: The glycolytic shift in fumarate-hydratase-deficient kidney cancer lowers AMPK levels, increases anabolic propensities and lowers cellular iron levels. Cancer Cell 20: 315-327, 2011.
21. Yuan SSF, Hou MF, Hsieh YC, Huang CY, Lee YC, Chen YJ and Lo S: Role of MRE11 in cell proliferation, tumor invasion, and DNA repair in breast cancer. J Natl Cancer Inst 104: 1485-1502, 2012.
22. Wang YY, Chen YK, Lo S, Chi TC, Chen YH, Hu SC, Chen YW, Jiang SS, Tsai FY, Liu W, *et al*: MRE11 promotes oral cancer progression through RUNX2/CXCR4/AKT/FOXA2 signaling in a nuclease-independent manner. Oncogene 40: 3510-3532, 2021.
23. Wang CH, Wang PJ, Hsieh YC, Lo S, Lee YC, Chen YC, Tsai CH, Chiu WC, Chu-Sung Hu S, Lu CW, *et al*: Resistin facilitates breast cancer progression via TLR4-mediated induction of mesenchymal phenotypes and stemness properties. Oncogene 37: 589-600, 2018.
24. Huang JY, Wang YY, Lo S, Tseng LM, Chen DR, Wu YC, Hou MF and Yuan SF: Visfatin mediates malignant behaviors through adipose-derived stem cells intermediary in breast cancer. Cancers (Basel) 12: 29, 2019.
25. Wang YY, Chen HD, Lo S, Chen YK, Huang YC, Hu SC, Hsieh YC, Hung AC, Hou MF and Yuan SF: Visfatin enhances breast cancer progression through CXCL1 induction in tumor-associated macrophages. Cancers (Basel) 12: 3526, 2020.
26. Udupa S, Nguyen S, Hoang G, Nguyen T, Quinones A, Pham K, Asaka R, Nguyen K, Zhang C, Elgogary A, *et al*: Upregulation of the glutaminase II pathway contributes to glutamate production upon glutaminase 1 inhibition in pancreatic cancer. Proteomics 19: 1800451, 2019.
27. Bardella C, Olivero M, Lorenzato A, Geuna M, Adam J, O'Flaherty L, Rustin P, Tomlinson I, Pollard PJ and Di Renzo MF: Cells lacking the fumarase tumor suppressor are protected from apoptosis through a hypoxia-inducible factor-independent, AMPK-dependent mechanism. Mol Cell Biol 32: 3081-3094, 2012.
28. Barker KT, Bevan S, Wang R, Lu YJ, Flanagan AM, Bridge JA, Fisher C, Finlayson CJ, Shipley J and Houlston RS: Low frequency of somatic mutations in the FH/multiple cutaneous leiomyomatosis gene in sporadic leiomyosarcomas and uterine leiomyomas. Br J Cancer 87: 446-448, 2002.
29. Kiuru M, Lehtonen R, Arola J, Salovaara R, Järvinen H, Aittomäki K, Sjöberg J, Visakorpi T, Knuutila S, Isola J, *et al*: Few FH mutations in sporadic counterparts of tumor types observed in hereditary leiomyomatosis and renal cell cancer families. Cancer Res 62: 4554-4557, 2002.

30. Sciacovelli M, Gonçalves E, Johnson TI, Zecchini VR, da Costa AS, Gaude E, Drubbel AV, Theobald SJ, Abbo SR, Tran MG, et al: Fumarate is an epigenetic modifier that elicits epithelial-to-mesenchymal transition. Nature 537: 544-547, 2016.
31. Schmidt C, Sciacovelli M and Frezza C: Fumarate hydratase in cancer: A multifaceted tumour suppressor. Semin Cell Dev Biol 98: 15-25, 2020.
32. Ge X, Li M, Yin J, Shi Z, Fu Y, Zhao N, Chen H, Meng L, Li X, Hu Z, et al: Fumarate inhibits PTEN to promote tumorigenesis and therapeutic resistance of type2 papillary renal cell carcinoma. Mol Cell 82: 1249-1260.e7, 2022.
33. Johnson TI, Costa AS, Ferguson AN and Frezza C: Fumarate hydratase loss promotes mitotic entry in the presence of DNA damage after ionising radiation. Cell Death Dis 9: 913, 2018.
34. Isaacs JS, Jung YJ, Mole DR, Lee S, Torres-Cabala C, Chung YL, Merino M, Trepel J, Zbar B, Toro J, et al: HIF overexpression correlates with biallelic loss of fumarate hydratase in renal cancer: Novel role of fumarate in regulation of HIF stability. Cancer Cell 8: 143-153, 2005.
35. Sullivan LB, Martinez-Garcia E, Nguyen H, Mullen AR, Dufour E, Sudarshan S, Licht JD, Deberardinis RJ and Chandel NS: The proto-oncometabolite fumarate binds glutathione to amplify ROS-dependent signaling. Mol Cell 51: 236-248, 2013.
36. Gonçalves E, Sciacovelli M, Costa ASH, Tran MGB, Johnson TI, Machado D, Frezza C and Saez-Rodriguez J: Post-translational regulation of metabolism in fumarate hydratase deficient cancer cells. Metab Eng 45: 149-157, 2018.
37. Chang YJ, Huang JY, Lin CH and Wang BY: Survival and treatment of lung cancer in Taiwan between 2010 and 2016. J Clin Med 10: 4675, 2021.
38. Wang BY, Huang JY, Cheng CY, Lin CH, Ko J and Liaw YP: Lung cancer and prognosis in Taiwan: A population-based cancer registry. J Thorac Oncol 8: 1128-1135, 2013.
39. Sciacovelli M and Frezza C: Fumarate drives EMT in renal cancer. Cell Death Differ 24: 1-2, 2017.
40. Hou C, Ishi Y, Motegi H, Okamoto M, Ou Y, Chen J and Yamaguchi S: Overexpression of CD44 is associated with a poor prognosis in grade II/III gliomas. J Neurooncol 145: 201-210, 2019.
41. Zhang JG, Xu C, Zhang L, Zhu W, Shen H and Deng HW: Identify gene expression pattern change at transcriptional and post-transcriptional levels. Transcription 10: 137-146, 2019.
42. Martin J, Herbert B and Hocevar B: Disabled-2 downregulation promotes epithelial-to-mesenchymal transition. Br J Cancer 103: 1716-1723, 2010.
43. Sun C, Yao X, Jiang Q and Sun X: miR-106b targets DAB2 to promote hepatocellular carcinoma cell proliferation and metastasis. Oncol Lett 16: 3063-3069, 2018.
44. Yang YF, Wang YY, Hsiao M, Lo S, Chang YC, Jan YH, Lai TC, Lee YC, Hsieh YC and Yuan SF: IMPAD1 functions as mitochondrial electron transport inhibitor that prevents ROS production and promotes lung cancer metastasis through the AMPK-Notch1-HEY1 pathway. Cancer Lett 485: 27-37, 2020.
45. He K, Guo X, Liu Y, Li J, Hu Y, Wang D and Song J: TUFM downregulation induces epithelial-mesenchymal transition and invasion in lung cancer cells via a mechanism involving AMPK-GSK3β signaling. Cell Mol Life Sci 73: 2105-2121, 2016.
46. Han SY, Jeong YJ, Choi Y, Hwang SK, Bae YS and Chang YC: Mitochondrial dysfunction induces the invasive phenotype, and cell migration and invasion, through the induction of AKT and AMPK pathways in lung cancer cells. Int J Mol Med 42: 1644-1652, 2018.
47. Wu SB, Wu YT, Wu TP and Wei YH: Role of AMPK-mediated adaptive responses in human cells with mitochondrial dysfunction to oxidative stress. Biochim Biophys Acta 1840: 1331-1344, 2014.
48. Godlewski J, Nowicki MO, Bronisz A, Nuovo G, Palatini J, De Lay M, Van Brocklyn J, Ostrowski MC, Chiocca EA and Lawler SE: MicroRNA-451 regulates LKB1/AMPK signaling and allows adaptation to metabolic stress in glioma cells. Mol Cell 37: 620-632, 2010.
49. Gongol B, Sari I, Bryant T, Rosete G and Marin T: AMPK: An epigenetic landscape modulator. Int J Mol Sci 19: 3238, 2018.